Electrical transport via variable range hopping in an individual multi-wall carbon nanotube

2008 J. Phys.: Condens. Matter 20 475207

(http://iopscience.iop.org/0953-8984/20/47/475207)

J. Phys.: Condens. Matter **20** (2008) 475207 (7pp) doi:10.1088/0953-8984/20/47/475207

Electrical transport via variable range hopping in an individual multi-wall carbon nanotube

Zishan Husain Khan[1,2,5], M Husain[3], T P Perng[4], Numan Salah[1] and Sami Habib[1]

[1] Center of Nanotechnology, King Abdul Aziz University, Jeddah, The Kingdom of Saudi Arabia
[2] Department of Applied Sciences and Humanities, Faculty of Engineering and Technology, Jamia Millia Islamia (Central University), New Delhi, India
[3] Department of Physics, Jamia Millia Islamia (Central University), New Delhi, India
[4] Department of Chemical Engineering and Materials Science, Yuan Ze University, Chung-Li 320, Taiwan

E-mail: zishan_hk@yahoo.co.in

Received 6 July 2008, in final form 18 August 2008
Published 6 November 2008
Online at stacks.iop.org/JPhysCM/20/475207

Abstract

E-beam lithography is used to make four leads on an individual multi-wall carbon nanotube for carrying out electrical transport measurements. Temperature dependence of conductance of an individual multi-wall carbon nanotube (MWNT) is studied over a temperature range of (297–4.8 K). The results indicate that the conduction is governed by variable range hopping (VRH) for the entire temperature range (297–4.8 K). This VRH mechanism changes from three dimensions (3D) to two dimensions (2D) as we go down to 70 K. Three-dimensional variable range hopping (3D VRH) is responsible for conduction in the temperature range (297–70 K), which changes to two-dimensional VRH for much lower temperatures (70–4.8 K). For 3D VRH, various Mott parameters such as density of states, hopping distance and hopping energy have been calculated. The 2D VRH mechanism has been applied for the temperature range (70–4.8 K) and, with the help of this model, the parameters such as localization length and hopping distance are calculated. All these parameters give interesting information about this complex structure, which may be useful for many applications.

(Some figures in this article are in colour only in the electronic version)

1. Introduction

Carbon nanotubes (CNTs) have generated a great deal of interest and scientific curiosity due to their many unique properties and potential applications [1]. CNTs offer intriguing possibilities for the fabrication of nanometer-scale molecular electronic devices [2]. They are also promising candidates for studying low-dimensional physics including band structures [3], electron–electron interactions [4], electron–lattice coupling [5] and electron localization [6]. Electrical transport properties of multi-wall carbon nanotubes (MWNTs) are expected to depend on their structures such as multiplicity, chirality, imperfection, etc. Since the discovery of CNTs, studies on the transport properties of CNTs [7, 8] involving electron–electron interactions have drawn a lot of attention. Most of these studies are reported on bulk CNT samples. From the bulk samples, only average properties can be obtained. On the other hand, experiments on individual nanotube samples may provide more precise and reliable information about the electrical transport mechanism. Tans *et al* [9] reported Coulomb blockade properties on a individual SWNT, indicating that the SWNT indeed act as genuine quantum wires. From the measurements on rope (bundle) SWNTs, reports on Coulomb blockade and Luttinger-liquid behavior are also available in the literature [10, 11]. Agrawal *et al* [12] demonstrated that ozone exposure of individual multi-walled

[5] Author to whom any correspondence should be addressed.

carbon nanotubes (CNTs) results in up to a threefold increase in CNT conductivity and 50% decrease in carrier transport activation energy. Their results suggested that controlled defect creation could be an attractive strategy to induce electrical conductivity increase in multi-walled CNTs for use in nanodevice wiring and related applications. Ebbesen *et al* [13] performed the first four-probe measurements of the individual MWNTs, which showed a great diversity in the conduction properties. Later on, both ballistic conduction [14, 15] and diffusive transport [16, 17] on individual MWNTs were reported. Measurements of the Aharonov–Bohm oscillation in MWNTs showed that the current flows only through the outermost shell [18]. Huang *et al* [19] reported the atomic-scale imaging with concurrent transport measurements of the breakdown of individual multi-wall carbon nanotubes inside a transmission electron microscope equipped with a piezo-manipulator. They observed a significant amount of current drop was observed when an innermost wall is broken, proving unambiguously that every wall is conducting. They also reported that the breakdown of each wall in any sequence initiates in the middle of the nanotube, not at the contact, proving that the transport is not ballistic. Cao *et al* [20] observed various low-temperature transport regimes in true-metallic, small- and large-bandgap semiconducting nanotubes, including quantum state shell-filling, -splitting and -crossing in magnetic fields owing to the Aharonov–Bohm effect. Their clean transport data showed a correlation between the contact junction resistance and the various transport regimes in single-walled carbon nanotube devices. Furthermore, they reported that electrical transport data can be used to probe the band structures of nanotubes, including nonlinear band dispersion. In another experiment Xu *et al* [21] proposed two device models of outer-wall disordered carbon nanotubes where lead contacts of multi- and single-wall nanotubes are proposed for both measurement and control of carrier mobility in multi-wall carbon nanotubes and found that the average conductance and localization length largely exceed those in the bulk disorder, showing the relative robustness of the model device to surface disorder. There are many reports available on electrical properties of carbon nanotube (CNT) film/bulk in the literature [22, 23], but only a few of them address the electrical transport properties of an individual CNT using the four-probe method, which can measure the intrinsic tube conductivity [24, 25].

In the present work, we have also studied the electrical transport properties of an individual MWNT to understand the conduction mechanism of this complex structure. We have observed the variable range hopping (VRH) type of conduction mechanism for the entire temperature range (297–4.8 K). The conduction takes place via three-dimensional variable range hopping (VRH) for the temperature region 297–70 K and, for the temperature range of 70–4.8 K, this VRH mechanism changes from three-dimensional to two-dimensional as we reduce the temperature to 70 K. Therefore, the data for the temperature region 297–70 K is plotted for the 3D VRH model, while, for the lower-temperature range (70–4.8 K), the 2D variable range hopping is found to give a good fit to the data. Applying this model, we have calculated various parameters such as density of states, hopping distance and hopping energy. These parameters give important information about this individual carbon nanotube.

2. Experimental procedure

Carbon nanotubes have been synthesized by a low pressure chemical vapor deposition (LPCVD) technique on an iron–palladium ($Fe_{70}Pd_{30}$) catalyst film. The reactive gas mixture is N_2:C_2H_2:H_2 with a flow rate of 300:50:50 sccm. The chamber pressure and temperature are maintained at 10 Torr. and 800 °C, respectively. The growth time is kept fixed at 1 h. A field emission scanning electron microscope (FESEM, JEOL 6500) is employed to observe the size and shape of Fe–Pd catalyzed carbon nanotubes. The structure of CNTs is confirmed by high-resolution transmission electron microscopy (HRTEM, JEOL-264 JEM 3011) at 300 kV. The amorphous structure of CNTs is verified by a Fourier-transformed (FT) Raman spectrometer (Bruker, RFS 100/S), using a Nd:YAG laser with an excitation wavelength of 1064 nm.

To study the electrical transport measurements of individual disordered MWNTs, we have used a conventional e-beam lithography technique to connect individual MWNT with fine leads of 1 μm. We have measured the temperature dependence of conductance using a standard method of ac bias current lock-in voltage detection. For the preparation of the sample for e-beam lithography, we have used a solution of MWNTs dispersed in acetone and then spread a small drop of this solution onto a specially designed electrode pattern made on a silicon (100) substrate coated with a silicon oxide layer 600 nm thick, as shown in figure 5. Using SEM, the dispersed MWNTs are first located and then a bilayer PMMA photoresist is spun over the sample followed by subsequent baking at 160 °C for 4–5 h inside an oven (figure 6(a)). After preparing the sample using this process, an e-beam lithography technique is used to define the pattern of fine leads on an individual MWNT using the process shown in figure 6(b). Once the e-beam exposure is over, the sample is taken out and developed, and finally the pattern is checked under a high-resolution optical microscope. Once the desired pattern is written, a 200 nm thin niobium (Nb) film is sputtered onto the sample. The sample is kept in acetone for a very short time to wash away the unwanted niobium (Nb) from the sample and finally we are left with the four electrodes on individual MWNTs. With the help of these electrodes, we have measured the resistance of the individual disordered MWNTs over a wide temperature range. Before starting the measurements, ohmic behavior is verified and a linear I–V curve is obtained. A standard method of ac bias current with lock-in voltage detection is employed to measure the resistance of the sample at different temperatures (297–4.8 K).

3. Results and discussion

The FESEM image of carbon nanotubes grown on a $Fe_{70}Pd_{30}$ film for 1 h growth time is presented in figure 1. The diameter of these carbon nanotubes varies from 40 to 90 nm.

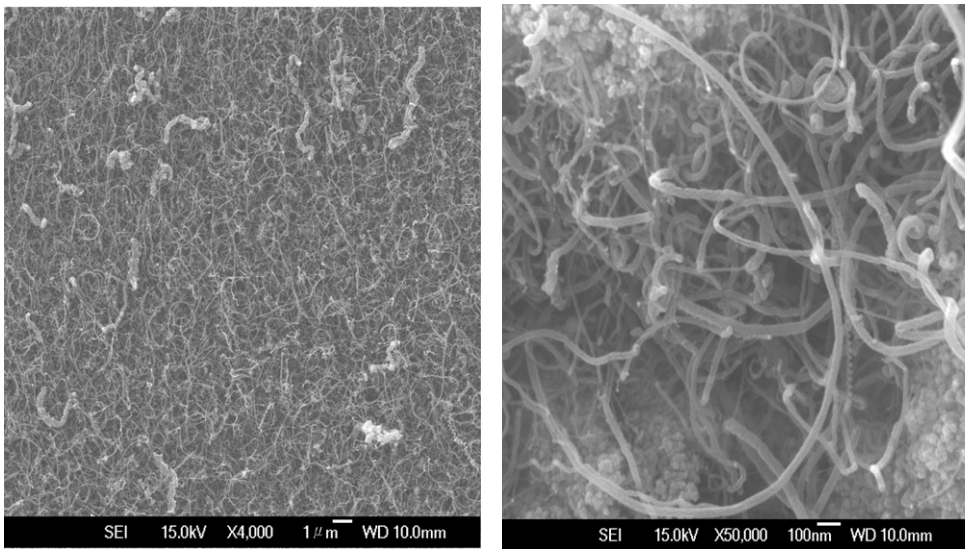

Figure 1. FESEM image of $Fe_{70}Pd_{30}$-catalyzed MWNTs.

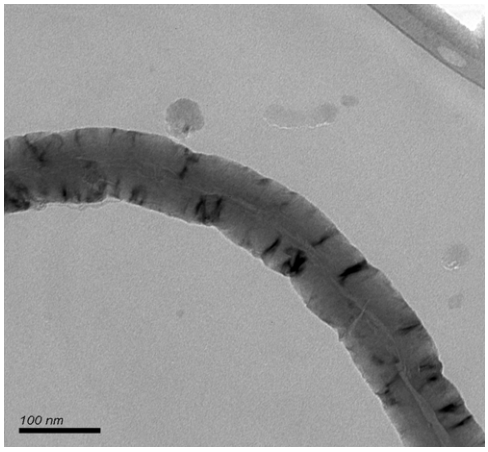

Figure 2. TEM image of $Fe_{70}Pd_{30}$-catalyzed MWNTs.

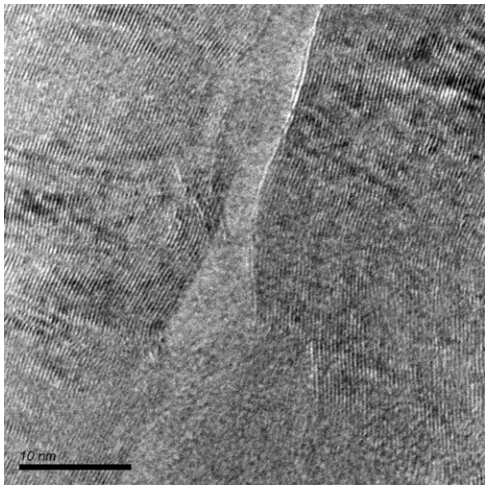

Figure 3. HRTEM image of $Fe_{70}Pd_{30}$-catalyzed MWNTs.

The TEM image of these CNTs shown in figure 2 reveals that these nanotubes are multi-walled and contain a lots of defects, thereby showing a disordered structure. Figure 3 shows the HRTEM image of the multi-wall carbon nanotube. As is evident from this image, these MWNTs do not possess a coaxial cylindrical structure, but contain a lot of defects, thereby showing a disordered structure. The graphene layers are also not parallel but look somewhat broken.

Raman spectroscopic measurement is also performed to confirm the amorphous structure of carbon nanotubes. Raman spectra of carbon nanotubes are presented in figure 4, which shows a sharp peak of the D-band and a weak peak of the G-band located at 1345 and 1580 cm^{-1}, respectively. These carbon nanotubes show a strong peak at 1350 cm^{-1} (roughly corresponding to the D-line associated with disorder-allowed zone-edge modes of graphite). Normally, the higher intensity of the 1350 cm^{-1} peak is an indication of an increased amount of amorphous carbon in the samples, which is in agreement with the HRTEM image.

Four leads on individual CNTs are presented in figure 7. The width of each lead is 1 μm with about 2 μm interspacing. The length and diameter of the connected individual MWNTs is about 15 μm and 80 nm, respectively.

Several models are available in the literature to explain the nonlinear behavior of conductance in CNTs. For MWNTs containing a lot of impurities or disorder, the mechanisms responsible for the decrease in conductance at lower temperatures include thermally activated transport, variable range hopping and weak localization [26–28]. For the present system of an individual MWNT, the temperature dependence of conductance for the temperature region 297–4.8 K is presented in figure 8. It is found that the entire data for the temperature region 297–4.8 K could also be fitted well with the help of a variable range hopping model. Here, we have explained the temperature dependence of conductance using variable range hopping for the entire temperature region (297–4.8 K).

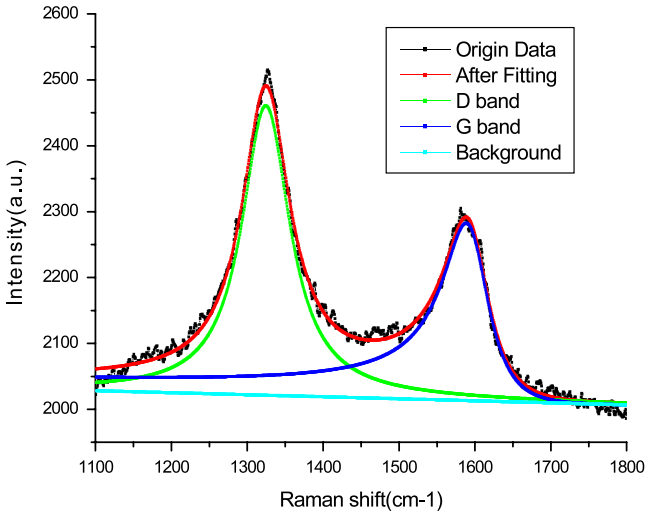

Figure 4. Raman spectra of $Fe_{70}Pd_{30}$-catalyzed MWNTs.

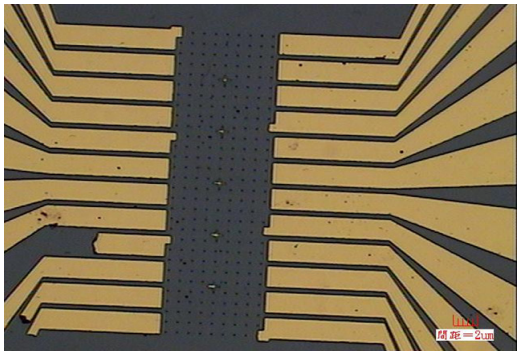

Figure 5. Pattern drawn on silicon wafer to connect individual CNTs.

The data have been fitted for three-as well as two-dimensional variable range hopping (VRH) for the entire temperature region (297–4.8 K). For the temperature range 297–70 K, it is observed that the 3D VRH is fitted well only up to a temperature of 70 K. Below 70 K, the 2D VRH model gives a good fit to the data for the present sample. The data is divided into two different ranges, i.e. 297–70 K for the 3D VRH model and 70–4.8 K for the 2D VRH model. Initially, for the temperature range 297–70 K, the data is re-plotted as $\ln G\sqrt{T}$ versus $T^{-1/4}$ for 3D variable range hopping (figure 9).

From the plot of $\ln G\sqrt{T}$ versus $T^{-1/4}$ it is observed that the conductance over the temperature region 297–70 K increases slowly with increasing temperature, which suggests that the conduction is due to variable range hopping which is characterized by the Mott [29–33] expression of the form

$$G = \frac{G_0'}{\sqrt{T}} \exp(-AT^{-1/4}) \tag{1}$$

where G is the conductance, G_0' is the pre-exponential factor and A is the constant, which is given as

$$A^4 = T_d = \frac{\lambda\alpha^3}{kN(E_F)} \tag{2}$$

$N(E_F)$ is the density of localized states at E_F, λ is a dimensionless constant (about 18), T_d is the degree of disorder, k is the Boltzmann constant and α^{-1} represents the spatial extension of the wavefunction $\exp(-\alpha R)$ associated with the localized states. It is given by

$$\alpha = 22.52G_0'A^2 \text{ cm}^{-1} \tag{3}$$

$$N(E_F) = 2.12 \times 10^9 G_0'^3 A^2 \text{ cm}^{-3} \text{ eV}^{-1}. \tag{4}$$

The hopping distance (R) is given by [29–33]

$$R = \left(\frac{9}{8\pi\alpha kTN(E_F)}\right)^{1/4} \tag{5}$$

where k is the Boltzmann constant and $N(E_F)$ is the density of localized states.

Hopping energy (W) is also given by [29–33]

$$W = \left(\frac{3}{4\pi R^3 N(E_F)}\right). \tag{6}$$

Hopping energy (W), in general, can be defined as the energy required for inelastic tunneling transfer of an electron between two localized electronic states centered at different locations or the energy required between two localized states with the assistance of phonons. We have calculated the parameters, such as density of states ($N(E_F)$), degree of disorder (T_d), hopping distance (R) and hopping energy (W) with the help of equations (3)–(6) and these parameters are called the Mott parameters. For variable range hopping, the value of W should be of the order of a few k_BT and αR should be greater than unity or of the order of unity, as suggested by Mott. The values of these Mott parameters are presented in table 1. It is evident from the table that the calculated values of W and αR are of the order of a few k_BT and unity, respectively, which shows close agreement with Mott's [29–33] variable range hopping. It is also observed that the hopping distance increases with the decrease in temperature, while the hopping energy (W) decreases with the decrease in temperature. The density of states near the Fermi level extracted from the VRH parameters is estimated to be 3.15×10^{23} eV^{-1} cm^{-3} for the present sample of individual MWNTs. The degree of disorder (T_d) is estimated to be 0.383×10^4 K. Various workers have reported a value of $T_d \approx 10^4$ K for plasma-polymerized C_{60} thin films [34] and on the basis of the value of T_d, they concluded that their system is disordered. In our case, the value of T_d is of the same order as that reported by these workers, indicating that the present sample is also disordered.

Aggarwal *et al* [35] studied the temperature dependence of electrical conductivity of $Fe_{70}Pt_{30}$-catalyzed MWNT films is done over a wide temperature range from 293 to 4 K. They have fitted the measured experimental data with variable range hopping (VRH) and interpreted the results using Mott's (VRH) model. They have also reported a crossover of conduction mechanism $Fe_{70}Pt_{30}$ catalyzed in this MWNT film from the $\exp[-(T_d/T)]^{1/4}$ law in the temperature range 293–110 K to $\exp[-(T_0/T)]^{1/3}$ in the low-temperature range (110–4 K). This behavior is attributed to a temperature-induced transition from three-dimensional (3D) to two-dimensional (2D) VRH.

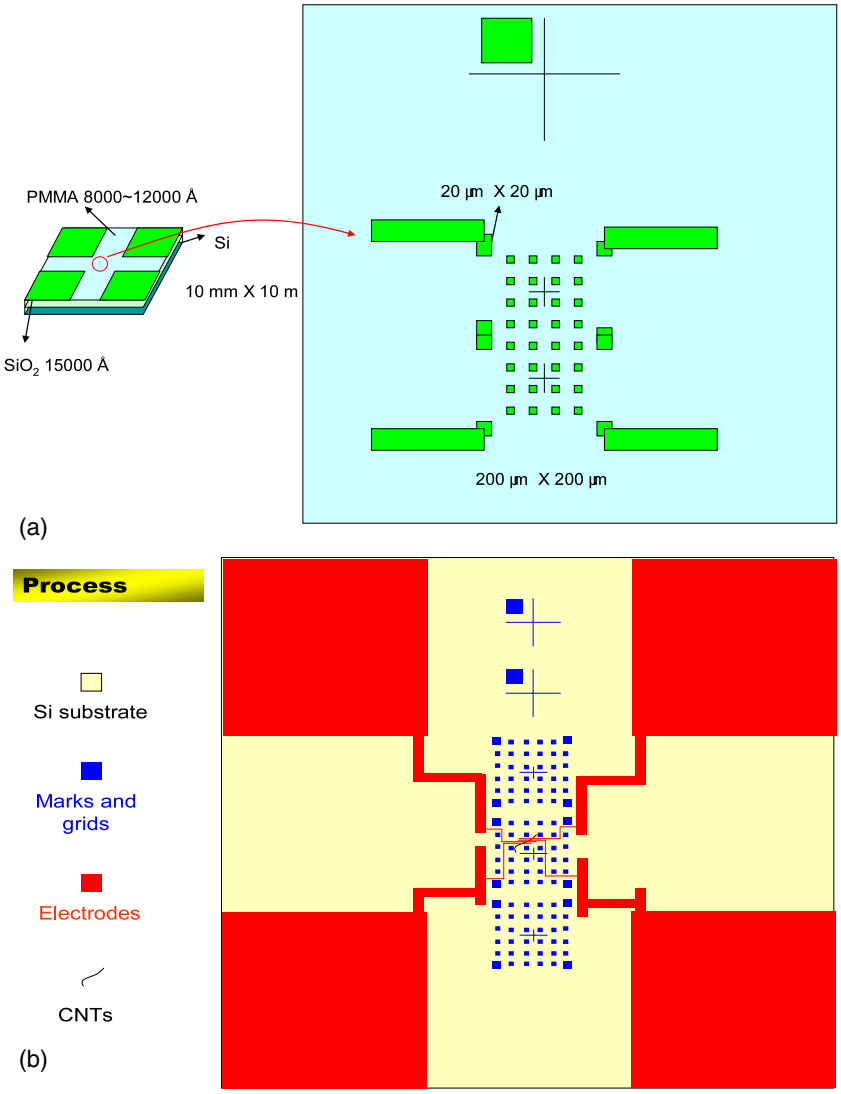

Figure 6. (a), (b) Process involved in connecting the individual CNT.

Table 1. The Mott parameters of an individual $Fe_{70}Pd_{30}$-catalyzed MWNT for temperature range 297–70 K.

T (K)	$N(E_F)$ (eV^{-1} cm^{-3})	T_d (K)	α (cm^{-1})	R (cm)	W (meV)	αR
297	3.15×10^{23}	0.383×10^4	1.867×10^7	3.93×10^{-6}	12.5	0.733
200	3.15×10^{23}	0.383×10^4	1.867×10^7	4.33×10^{-6}	9.34	0.808
150	3.15×10^{23}	0.383×10^4	1.867×10^7	4.66×10^{-6}	7.503	0.869
100	3.15×10^{23}	0.383×10^4	1.867×10^7	5.15×10^{-6}	5.535	0.962
70	3.15×10^{23}	0.383×10^4	1.867×10^7	5.64×10^{-6}	4.24	1.052

Various Mott parameters like characteristic temperature (T_0), density of states at the Fermi level $N(E_F)$, localization length (ξ), hopping distance (R) and hopping energy (W) have also been calculated using the above-mentioned model. Aggarwal *et al* [36] reported the electrical transport measurements of $Fe_{70}Pd_{30}$-catalyzed MWNT films over a temperature range of 298–4.2 K. The results have been interpreted in terms of variable range hopping (VRH) over the entire temperature range of 298–4.2 K. Three-dimensional variable range hopping ($\ln G\sqrt{T}$ versus $T^{-1/4}$ fitting) is suggested for the temperature range 298–125 K, while two-dimensional variable range hopping ($\ln G\sqrt{T}$ versus $T^{-1/3}$ fitting) is observed for the temperature range 125–4.2 K. On the basis of experimental data fitting, they have also calculated various parameters such as characteristic temperature (T_0), density of states at the Fermi level $N(E_F)$, localization length (ξ), hopping distance (R) and hopping energy (W). In the present work, we have isolated individual $Fe_{70}Pd_{30}$-catalyzed multi-walled carbon nanotubes from the bulk MWNT film and reported the electrical transport properties of this individual multi-walled carbon nanotube. It is understood the properties studied on individual $Fe_{70}Pd_{30}$-catalyzed carbon nanotubes will be more

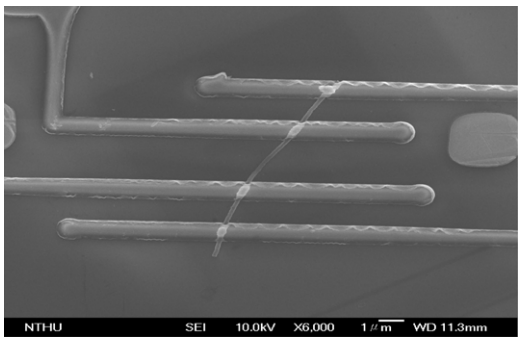

Figure 7. Four leads on an individual $Fe_{70}Pd_{30}$-catalyzed MWNT.

precise and meaningful than that of the bulk sample (CNT film). From the carbon nanotube film, we can determine only average properties of the material, which is not very precise as it may contain a number of unwanted impurities. These impurities may also influence the electrical transport properties of the bulk sample of multi-walled carbon nanotubes. On the basis of the present work on individual $Fe_{70}Pd_{30}$-catalyzed multi-walled carbon nanotubes, it is clear that this nanotube is more disordered and thereby shows a VRH type of conduction mechanism. The values of electrical parameters calculated in the present work are comparable with our earlier reported results.

For the lower-temperature region of 70–4.8 K, the conductance is further suppressed and increases very slowly with increasing temperature, suggesting that conduction is due to 2D variable range hopping in localized states near the Fermi level. Therefore, the data have been re-plotted as $\ln G\sqrt{T}$ versus $T^{-1/3}$ for 2D VRH.

The plot of $\ln G\sqrt{T}$ versus $T^{-1/3}$ in the temperature range 70–4.8 K is presented in figure 10. This figure shows that all the data points almost form a straight line, indicating that conductance (G) obeys the following equation:

$$G \cdot \sqrt{T} = G_0 \cdot \exp\left[-\left(\frac{T_0}{T}\right)^{1/3}\right] \tag{7}$$

where G is the conductance, G_0 is the pre-exponential factor and T_0 is the characteristic temperature.

The linear behavior of the $\ln G\sqrt{T}$ versus $T^{-1/3}$ plot suggests that the conduction is due to Mott's two-dimensional (2D) non-interacting variable range hopping, which is consistent with the amorphous structure of the present sample of MWNTs. The HRTEM image shown in figure 3 also suggests that the carbon nanotubes do not possess long-range order, but they contain imperfect and broken graphite layers of varying sizes. Gao *et al* also reported the similar observations for multi-walled carbon nanotubes [37]. Therefore it is suggested that the transport along a continuous single shell or set of shells, as in the case of MWNTs, is impossible and only the disordered structure of MWNTs plays an important role. Therefore, it may be suggested that the disorder localizes the electronic wavefunction, thus giving rise to variable range hopping.

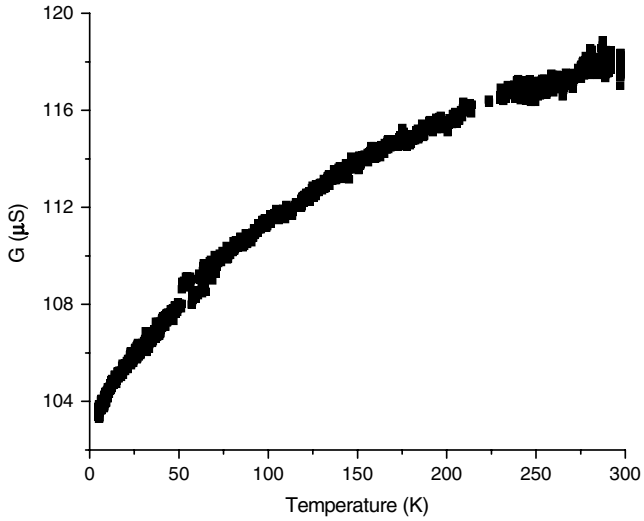

Figure 8. Conductance (G) versus temperature (K) for an individual $Fe_{70}Pd_{30}$-catalyzed MWNT for the temperature range 297–4.8 K.

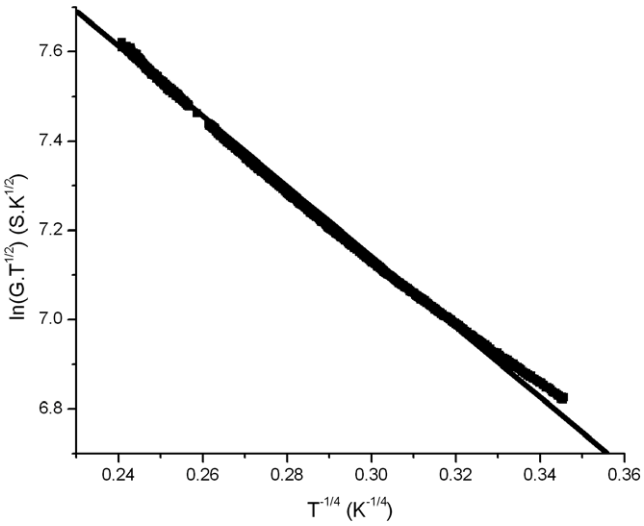

Figure 9. $\ln(G\sqrt{T})$ versus $T^{-1/4}$ plot of an individual $Fe_{70}Pd_{30}$-catalyzed MWNT for the temperature range 297–70 K.

In the two-dimensional variable range hopping regime, the characteristic temperature (T_0) is related to the density of states at the Fermi level $N(E_F)$ and the localization length ξ as [38]

$$T_0 = \frac{13.8}{k_B N(E_F)\xi^2}. \tag{8}$$

The temperature dependence of the optimum hopping distance ($R(T)$) is given by

$$R(T) = \frac{1}{3}\xi\left(\frac{T_0}{T}\right)^{1/3}. \tag{9}$$

The localization length and the optimum hopping distance for this disordered MWNT have been estimated using equations (8) and (9). We have used the value of $N(E_F)$ estimated using 3D VRH as suggested by earlier workers [39] to calculate the localization length and hopping distance. The

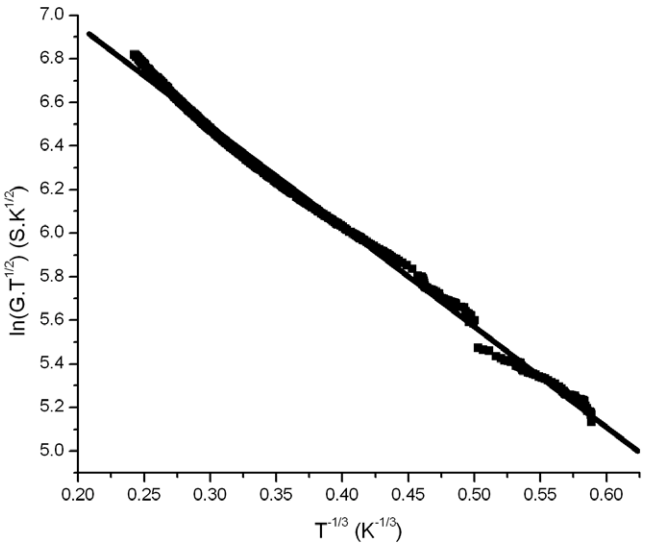

Figure 10. $\ln(G\sqrt{T})$ versus $T^{-1/3}$ plot of an individual $Fe_{70}Pd_{30}$-catalyzed MWNT for the temperature range 70–4.8 K.

localization length is calculated to be 0.72×10^{-10} cm using the value of T_0 and the density of states $N(E_F)_{3D}$. This gives an optimum hopping distance of 0.269×10^{-10} cm and 0.647×10^{-10} cm at 70 and 4.8 K, respectively.

4. Conclusion

It is concluded that, for the present sample of an individual MWNT, variable range hopping (VRH) is responsible for the transport of charge carriers. It is suggested that the hopping conduction takes place over the entire temperature range of 297–4.8 K. The VRH is responsible for the transport of charge carriers for the temperature range of 297–4.8 K. This variable range hopping changes from 3D to 2D for the lower-temperature region (70–4.8 K). Using the 3D VRH model, the calculated values of Mott parameters for the present sample of MWNTs satisfy the condition of Mott's variable range hopping (W of the order of a few k_BT and αR should be of the order of or greater than unity). For this individual MWNT, the hopping distance has also been calculated using the 2D VRH model, which varies from 0.269×10^{-10} to 0.647×10^{-10} as the temperature decreases from 70 to 4.8 K.

References

[1] Iijima S 1991 *Nature* **354** 56
[2] Frank S, Poncharal P, Wang Z L and de Heer W A 1998 *Science* **280** 1744
[3] Dresselhaus M S, Dresselhaus G and Eklund P C 1996 *Science of Fullerenes and Carbon Nanotubes* (San Diego, CA: Academic)
[4] Kane C, Balents L and Fisher M P A 1997 *Phys. Rev. Lett.* **79** 5086
[5] Kane C L and Mele E J 1997 *Phys. Rev. Lett.* **78** 1932
[6] White C T and Todorov T N 1998 *Nature* **393** 240
[7] Ogata M and Fukuyama H 1994 *Phys. Rev. Lett.* **73** 468
[8] Graugnard E, de Pablo P J, Walsh B, Ghosh A W, Datta S and Reifenberger R 2001 *Phys. Rev.* B **64** 125407
[9] Tans S J, Devort M H, Dai H, Thess A, Smalley R E, Geerligs L J and Dekker C 1997 *Nature* **386** 474
[10] Bockrath M, Cobden D H, McEuen P L, Chopra N G, Zettl A, Thess A and Smalley R E 1997 *Science* **275** 1922
[11] Yosida Y and Oguro I 1999 *J. Appl. Phys.* **86** 999
[12] Agrawal M, Raghuveer S, Li H and Ramanath G 2007 *Appl. Phys. Lett.* **90** 193104
[13] Ebbesen T W, Lezec H J, Hiura H, Bennett J W, Ghaemi H F and Thio T 1996 *Nature* **382** 54
[14] Frank S, Poncharal P, Wang Z L and de Heer W A 1998 *Science* **280** 1744
[15] Sanvito S, Kwon Y-K, Tománek D and Lambert C J 2000 *Phys. Rev. Lett.* **84** 1974
[16] Langer L, Bayot V, Grivei E, Issi J-P, Heremans J P, Olk C H, Stockman L, Van Haesendocnk C and Bruynserade Y 1996 *Phys. Rev. Lett.* **76** 479
[17] Bachtold, Strunk C, Salevetat J-P, Bonard J-M, Forró L, Nussbaumer T and Schoïenberger C 1999 *Nature* **397** 673
[18] Altshuler B L and Aronov A G 1979 *Solid State Commun.* **30** 115
[19] Huang J Y, Chen S, Jo S H, Wang Z, Han D X, Chen G, Dresselhaus M S and Ren Z F 2005 *Phys. Rev. Lett.* **94** 236802
[20] Cao J, Wang Q and Dai H 2005 *Nat. Mater.* **4** 745
[21] Xu N, Ding J W and Xing D Y 2008 *J. Appl. Phys.* **103** 083710
[22] Choi E S, Brooks J S, Eaton D L, Al-Haik M S, Hussaini Y, Garmestani H, Li D and Dahman K 2003 *J. Appl. Phys.* **94** 6034
[23] Wei B, Spolenak R, Redlich P K, Ruhle M and Arzt E 1999 *Appl. Phys. Lett.* **74** 3149
[24] Hsiou Y F, Yang Y J, Stobinski L, Kuo W and Chen C D 2004 *Appl. Phys. Lett.* **84** 984
[25] Balasubramanian K, Fan Y, Burghad M and Kern K 2004 *Appl. Phys. Lett.* **84** 2400
[26] Jang W Y, Kulkarni N N, Shih C K and Yao Z 2004 *Appl. Phys. Lett.* **84** 1177
[27] Kong J, Zhou C, Morpurgo A, Soh H T, Quate C F, Marcus C and Dai H 1999 *Appl. Phys.* A **69** 305
[28] Khan Z H, Malik M M, Zulfequar M and Husain M 1995 *J. Phys.: Condens. Matter* **7** 8979
[29] Mott N F and Davis E A 1970 *Electronic Processes in Non-Crystalline Materials* (Oxford: Clarendon)
[30] Mott N F 1970 *Phil. Mag.* **22** 7
[31] Mott N F and Davis E A 1970 *Phil. Mag.* **22** 903
[32] Mott N F 1975 *Phil. Mag.* **32** 961
[33] Mott N F 1969 *Phil. Mag.* **19** 835
[34] Shiraishi M, Ramm M and Ata M 2002 *Appl. Phys.* A **74** 613
[35] Aggarwal M, Khan S, Husain M, Ming T C, Tsai M Y, Perng T P and Khan Z H 2007 *Eur. Phys. J.* B **60** 319
[36] Aggarwal M, Husain M, Khan S and Khan Z H 2007 *J. Nanopart. Res.* **9** 1047
[37] Gao H, Mu C, Wang F, Xu D, Wu K, Xie Y, Liu S, Wang E, Xu J and Yu D 2003 *J. Appl. Phys.* **93** 5602
[38] Shklovskii B I and Efros A L 1984 *Electronic Properties of Doped Semiconductors* (Berlin: Springer)
[39] Jang W Y, Kulkarni N N, Shih C K and Yao Z 2004 *Appl. Phys. Lett.* **84** 1177